




Synthesis and catalytic properties of an iron(III) complex supported by amine-bis(phenolate) ligand

Yun-Xiao Zhang, Ling-Zhi Fu, Ling-Ling Zhou, Ling-Zhi Tang & Shu-Zhong Zhan

To cite this article: Yun-Xiao Zhang, Ling-Zhi Fu, Ling-Ling Zhou, Ling-Zhi Tang & Shu-Zhong Zhan (2015) Synthesis and catalytic properties of an iron(III) complex supported by amine-bis(phenolate) ligand, Journal of Coordination Chemistry, 68:13, 2286-2295, DOI: 10.1080/00958972.2015.1050005

To link to this article: <http://dx.doi.org/10.1080/00958972.2015.1050005>

 View supplementary material 

 Accepted author version posted online: 21 May 2015.
Published online: 22 Jun 2015.

 Submit your article to this journal 

 Article views: 64

 View related articles 

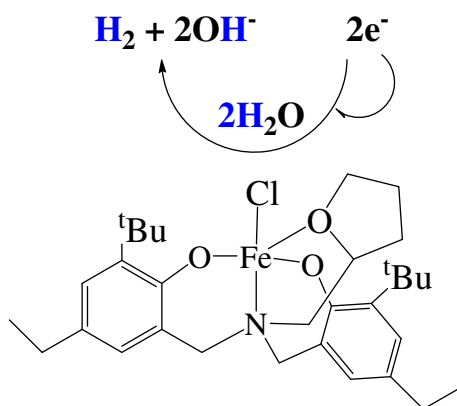
 View Crossmark data 

Synthesis and catalytic properties of an iron(III) complex supported by amine-bis(phenolate) ligand

YUN-XIAO ZHANG, LING-ZHI FU, LING-LING ZHOU, LING-ZHI TANG and SHU-ZHONG ZHAN*

College of Chemistry and Chemical Engineering, South China University of Technology, Guangzhou, China

(Received 14 February 2015; accepted 21 April 2015)



The reaction of FeCl_3 with 2-tetrahydrofuranyl-amino-N,N-bis(2-methylene-4-ethyl-tert-butylphenol), $\text{H}_2[\text{O}_3\text{N}]^{\text{BUeTHF}}$ (H_2L) affords a new iron(III) complex, $[\text{LFeCl}]$ **1**, whose structure has been determined by X-ray crystallography. Electrochemical studies show that **1** can electrocatalyze hydrogen evolution both from acetic acid with a turnover frequency (TOF) of 39.98 mol of hydrogen per mole of catalyst per hour at an overpotential of 941.6 mV (in DMF) and water with a TOF of 284.29 mol of hydrogen per mole of catalyst per hour at an overpotential of 896.8 mV (in buffer, pH 7.0). Sustained water reduction catalysis occurs at glassy carbon to give H_2 over a 2 h electrolysis period with 95.81% faradaic yield and no observable decomposition of the catalyst.

Keywords: Iron-complex; Molecular electrocatalyst; Water reduction; Hydrogen evolution

1. Introduction

Hydrogen is one of the most ideal energy carriers that can be an alternative to fossil fuels because of its numerous advantages, such as recyclability and pollution-free use [1]. Water

*Corresponding author. Email: shzhzhan@scut.edu.cn

splitting is an ideal method for hydrogen evolution in high purity and large quantities [2]. Effective proton reduction to form H₂ has been a subject of intense study, and significant effort has been made to design metal complexes for proton reduction [3]. Hydrogenases are very efficient catalysts for reductive generation or oxidative uptake of dihydrogen [4]. However, enzymes are difficult to obtain in sufficient amounts to adapt for commercial applications and their stability is often limited outside of their native environment [5, 6]. Electrolysis of water is the simplest way to produce hydrogen. To increase the reaction rate and decrease energy consumption, it is necessary to employ an efficient hydrogen evolution reaction electrocatalyst. Many research groups have focused on the development of molecular catalysts employing more transition metals, and several complexes that contain nickel [7, 8], cobalt [9–11], iron [12–14], copper [15–20], and molybdenum [21–25] have been developed as electrocatalysts for reduction of water to form H₂. Although, there has been significant progress in designing molecular catalysts for H₂ evolution, the search for highly active catalysts that can operate in aqueous solution still remains a challenge. In general, iron(III) complexes are employed as electrocatalysts for water oxidation [26–30], but there are few reports on water reduction by iron(III) complexes [31]. Herein, we present the synthesis and characterization of an iron complex, [LFeCl] **1**, as well as its catalytic properties.

2. Experimental

2.1. Materials and physical measurements

2-Tetrahydrofuranyl-amino-N,N-bis(2-methylene-4-ethyl-6-tert-butylphenol), H₂[O₃N]^{BuEtTHF} (H₂L) was prepared based on literature methods [32]. Elemental analyses for C, H, and N were obtained on a Perkin-Elmer analyzer model 240. Cyclic voltammograms (CVs) were obtained on a CHI-660E electrochemical analyzer under N₂ using a three-electrode cell in which a glassy carbon electrode gas chromatograph (GC) (1 mm in diameter) was the working electrode, a saturated Ag/AgNO₃ electrode was the reference electrode, and platinum wire was the auxiliary electrode. A ferrocene/ferrocenium (1+) couple was used as an internal standard; 0.10 M [(*n*-Bu)₄N]ClO₄ was used as the supporting electrolyte. Controlled-potential electrolysis (CPE) in aqueous media was conducted using an air-tight glass double compartment cell separated by a glass frit. The working compartment was fitted with a glassy carbon plate and a Ag/AgCl reference electrode. The auxiliary compartment was fitted with a Pt gauze electrode. The working compartment was filled with 50 mL of 0.25 M phosphate buffer solution, while the auxiliary compartment was filled with 35 mL phosphate buffer solution. After addition of iron complex, both compartments were sparged for 60 min with N₂ and CVs were recorded as controls. After electrolysis, a 0.5 mL aliquot of the headspace was removed and replaced with 0.5 mL of CH₄. A sample of the headspace was injected into the GC. GC experiments were carried out with an Agilent Technologies 7890A gas chromatography instrument.

2.2. Synthesis of complex, [LFeCl] **1**

To a solution, containing H₂L (0.481 g, 1 mmol) and triethylamine (0.2 g, 2 mmol) in THF (10 mL), FeCl₃ (0.162 g, 1 mmol) in methanol was added and the mixture was stirred for 15 min. Single crystals were obtained from the filtrate which was allowed to stand at room

temperature for several days, collected by filtration, and dried *in vacuo* (0.285 g, 81%). The elemental analysis results (found C 65.34; H 6.94; N 2.44%. C₃₁H₄₅ClFeNO₃ requires C 65.15; H 7.88; N 2.45%) were in agreement with the formula of the sample used for X-ray analysis.

2.3. Crystal structure determination

The X-ray analysis of **1** was carried out with a Bruker SMART CCD area detector using graphite monochromated Mo-K α radiation ($\lambda = 0.71073$ Å) at room temperature. All empirical absorption corrections were applied using SADABS [33]. The structure was solved using direct methods and the corresponding nonhydrogen atoms were refined anisotropically. All the hydrogens of the ligands were placed in calculated positions with fixed isotropic thermal parameters and included in the structure factor calculations in the final stage of full matrix least squares refinement. All calculations were performed using the SHELXTL computer program [34]. Table 1 lists details of the crystal parameters, data collection, and refinement for **1**. Selected bond distances are listed in table 2.

Table 1. Crystallographic data for **1**.

Parameter	Complex 1
Empirical formula	C ₃₁ H ₄₅ NO ₃ FeCl
Formula weight (g mol ⁻¹)	571.01
Temperature (K)	296.15
Crystal system	Monoclinic
Space group	<i>P</i> 2 ₁ / <i>n</i>
<i>a</i> (Å)	10.0876(9)
<i>b</i> (Å)	25.752(2)
<i>c</i> (Å)	12.8014(10)
α (°)	90.00
β (°)	94.474(2)
γ (°)	90.00
Volume (Å ³)	3315.4(5)
<i>Z</i>	4
Calculated density (g cm ⁻³)	1.1439
μ (mm ⁻¹)	0.563
<i>F</i> (0 0 0)	1222.5
Radiation	Mo-K α ($\lambda = 0.71073$)
2 θ range for data collection (°)	5.14–50.06
Index ranges	$-12 \leq h \leq 13$, $-31 \leq k \leq 33$, $-16 \leq l \leq 16$
Reflections collected	22,337
Independent reflections	5784 [$R_{\text{int}} = 0.0353$, $R_{\text{sigma}} = 0.0459$]
Data/restraints/parameters	5784/0/333
Goodness-of-fit on F^2	1.160
Final <i>R</i> indexes [$I \geq 2\sigma(I)$]	$R_1 = 0.0701$, $wR_2 = 0.2296$
Final <i>R</i> indexes [all data]	$R_1 = 0.0919$, $wR_2 = 0.2596$
Largest diff. peak/hole (e Å ⁻³)	1.52/–0.47

Table 2. Selected bond distances (Å) for **1**.

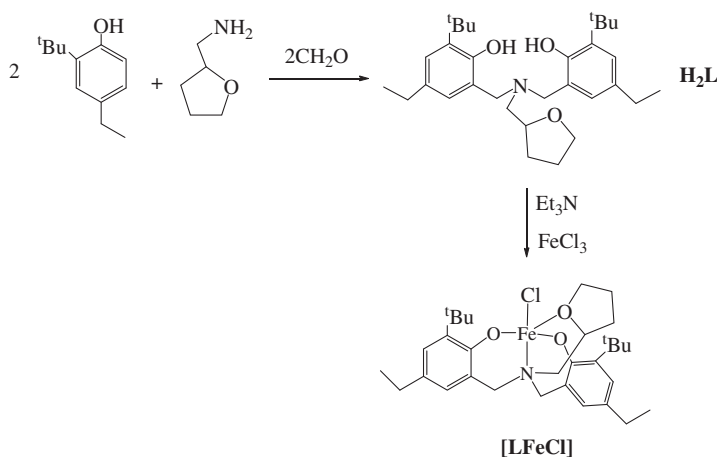
Fe1–O3	2.078(3)	Fe1–N9	2.251(3)
Fe1–O5	1.837(3)	Fe1–C11	2.2739(13)
Fe1–O7	1.840(3)		

3. Results and discussion

3.1. General characterization and crystal structure

In the presence of trimethylamine, reaction of FeCl_3 and H_2L provides an iron(III) complex, $[\text{LFeCl}]$ **1** (yield = 81%) (scheme 1), which is soluble in organic solvents, such as MeCN and CH_2Cl_2 .

As shown in figure 1, Fe(III) consists of two phenolate oxygens, O(5) and O(7), one tetrahydrofurfurylamine donor, O(3), one dimethylamino donor, N(9), and one Cl^- . The Fe(1)–O(5) distance of 1.837(3) Å and Fe(1)–O(7) length of 1.840(3) Å are similar to the iron–phenolate oxygen donor lengths observed in a related trigonal bipyramidal iron(III) complex possessing diamine-bis(phenolate) ligands bearing 2,4-dimethylsubstituted aromatic groups (abbreviated $\text{FeCl}[\text{O}_2\text{NN}]^{\text{MeMeNMe}_2}$) [35]. The Fe(1)–Cl(1) bond distance



Scheme 1. Schematic representation of the synthesis of $[\text{LFeCl}]$ **1**.

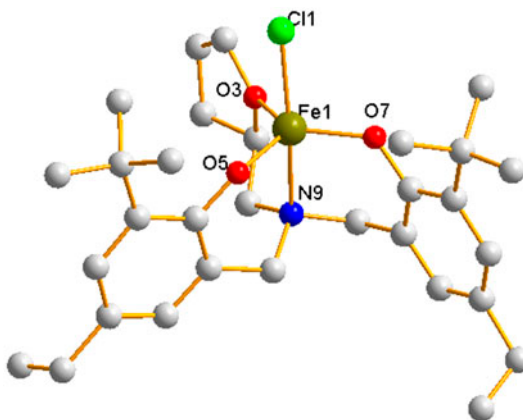


Figure 1. Molecular structure (ORTEP) of **1**.

of 2.2739(9) Å in **1** is similar to Fe–Cl bonds in octahedral iron(III) complexes possessing similar tetradentate ligands [36].

3.2. Cyclic voltammetry studies

CV of a DMF solution of **1** shows two reversible redox peaks at 0.16 and -0.37 V, and a quasi-reversible wave at -1.62 V, which are assigned to the couples of $\text{Fe}^{\text{III}}/\text{Fe}^{\text{II}}$, $\text{Fe}^{\text{II}}/\text{Fe}^{\text{I}}$, and $\text{Fe}^{\text{I}}/\text{Fe}^{\text{0}}$, respectively (figure 2). The current responses of the redox events at -0.37 and -1.62 V show linear dependence on the square root of the scan rate (figure S1 [see online supplemental material at <http://dx.doi.org/10.1080/00958972.2015.1050005>]), indicative of a diffusion-controlled process, with the electrochemically active species freely diffusing in solution.

From figure 3, it can be seen that the catalytic current near -1.65 V increased with increase in proton concentration (acetic acid concentration increased from 0.0 to

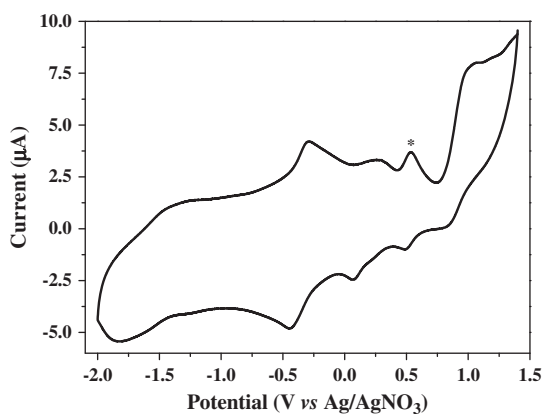


Figure 2. CV of 1.0 mM **1** in 0.10 M of $[n\text{-Bu}_4\text{N}]\text{ClO}_4$ DMF solution at a glassy carbon electrode and a scan rate of 100 mV s^{-1} . Ferrocene internal standard (*).

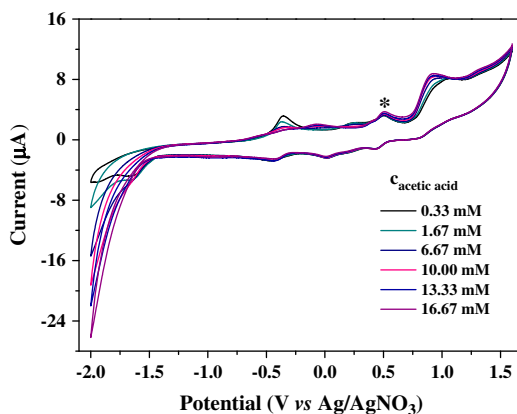


Figure 3. CVs of a 1.87 mM solution of **1** with varying concentrations of acetic acid in DMF. Conditions: r. t, 0.10 M $[n\text{-Bu}_4\text{N}]\text{ClO}_4$ as supporting electrolyte, scan rate: 100 mV s^{-1} , GC working electrode (1 mm diameter), Pt counter electrode, Ag/AgNO_3 reference electrode, Ferrocene internal standard (*).

16.67 mM). This indicates that hydrogen evolution electrocatalyzed by **1** requires the reduction of Fe^{I} to Fe^0 and protonation. Interestingly, with the acetic acid concentration increased from 0.0 to 16.67 mM (figure 3), the onset of the catalytic wave remains almost constant at *ca.* -1.45 V. Based on the above observations, the couple $\text{Fe}^{\text{I}}/\text{Fe}^0$ is also devoted to proton reduction. This result is different from a previous report that only couple $\text{Fe}^{\text{II}}/\text{Fe}^{\text{I}}$ is devoted to proton reduction [37]. Further mechanistic studies are under investigation.

Several control experiments were then carried out to confirm that **1** was responsible for the catalytic reaction. In particular, the free ligand, FeCl_3 , and mixture of the free ligand and FeCl_3 were each measured under identical conditions. As can be seen in figures S2–S5, the catalytic competency achieved with **1** is not matched by just ligand and FeCl_3 . Thus, a combination of the iron ion and the ligand is essential for catalytic activity.

3.3. Catalytic hydrogen evolution from acetic acid in DMF

Further evidence for the electrocatalytic activity was obtained by bulk electrolysis of a DMF solution of **1** ($0.714 \mu\text{M}$) with acetic acid (16.67 mM) at variable applied potential using a glassy carbon plate electrode in a double-compartment cell. Figure 4(a) shows the

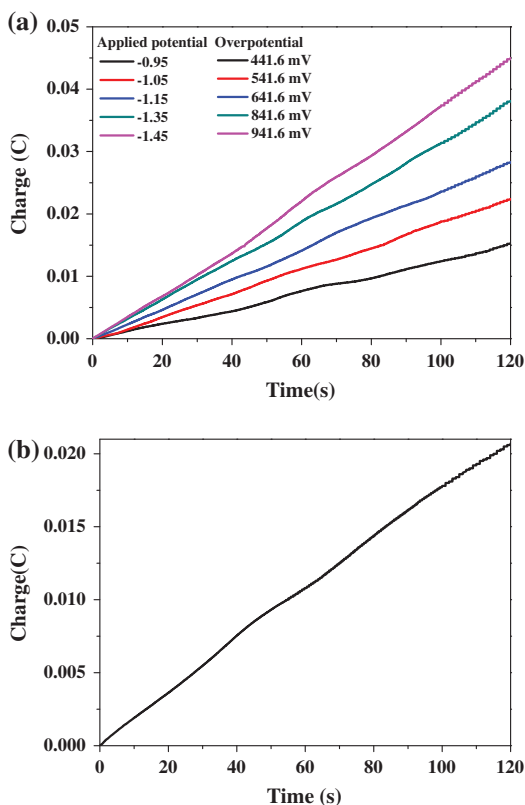


Figure 4. (a) Charge buildup vs. time from electrolysis of a $1.714 \mu\text{M}$ **1** in DMF ($0.10 \text{ M } [\text{n-Bu}_4\text{N}]\text{ClO}_4$) under various applied potentials. All data have deducted the blank. (b) Charge buildup vs. time from electrolysis of $0.10 \text{ M } [\text{n-Bu}_4\text{N}]\text{ClO}_4$ solution in DMF under $-1.45 \text{ V vs. Ag}/\text{AgNO}_3$.

total charge of bulk electrolysis of **1** in the presence of acid, the charge significantly increased when the applied potentials were set to more negative. When an applied potential was -1.45 V versus Ag/AgNO₃, the maximum charge reached 45 mC during 2 min of electrolysis. CPE under the same potential with a catalyst-free solution only gave a charge of 20 mC [figure 4(b)], indicating that this iron complex serves for effective hydrogen production under such conditions. Assuming every catalyst molecule was distributed on the electrode surface and every electron was used for the reduction of protons, according to equation (1) [8], we calculated turnover frequency (TOF) for the catalyst reaching a maximum of 39.98 mol of hydrogen per mole of catalyst per hour with an overpotential of 941.6 mV (equation S1 and figure S6).

$$\text{TOF} = \Delta C / (F \times n_1 \times n_2 \times t) \quad (1)$$

where ΔC is the charge from catalyst solution during CPE minus charge from solution without catalyst during CPE, F is the Faraday's constant, n_1 is the mol of electrons required to generate a mol of H₂, n_2 is the mol of catalyst in solution, and t is the duration of electrolysis.

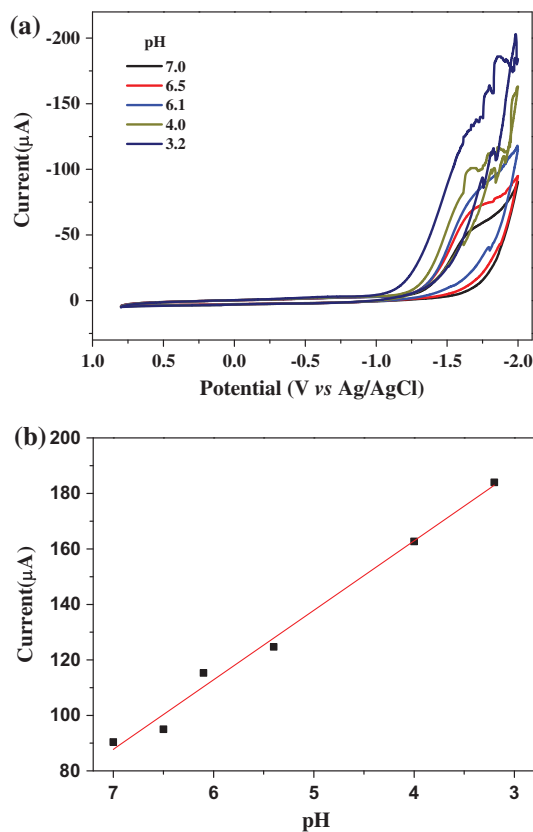


Figure 5. (a) CVs of 1.75 μM **1** showing variation in catalytic current with pH (scan rate: 100 mV s⁻¹). (b) Plot of catalytic peak current vs. pH.

3.4. Catalytic hydrogen evolution in aqueous media

To explore the catalytic hydrogen evolution in aqueous media, a much more attractive medium for the sustainable generation of hydrogen, CVs were measured in buffers at different pH values. Figure 5 exhibits a systematic increase in i_{cat} with decrease in pH from 7.0 to 3.2, suggesting that water reduction to H_2 occurs with **1** [9]. Further evidence for the electrocatalytic activity of **1** was also obtained by bulk electrolysis of an aqueous solution of **1** ($1.75 \mu\text{M}$) with buffer (0.10 M) at variable potential using a GC electrode in a double-compartment cell. When the applied potential was -1.45 V versus Ag/AgCl , the maximum charge was only 4 mC during 2 min of electrolysis in the absence of **1** [figure 6(a)], under the same conditions, the charge reached 327 mC [figure 6(b)], accompanying the formation of a large amount of gas bubbles, can be attributed to the catalytic generation of H_2 from water. The evolved H_2 was analyzed by gas chromatography [figure S7(a)], which gave 4.95 mL of H_2 over an electrolysis period of 2 h with a faradaic efficiency of 95.81% for H_2 [figure S7(b)]. According to equation (1), we also calculated TOF for the catalyst reaching a maximum of 284.29 mol of hydrogen per mole of catalyst per hour with an overpotential of 896.8 mV (figure S8).

To prove **1** as a homogeneous electrocatalyst, we obtained dependence of the catalytic current on concentration of **1**. As shown in figure S9, the observation of the catalytic

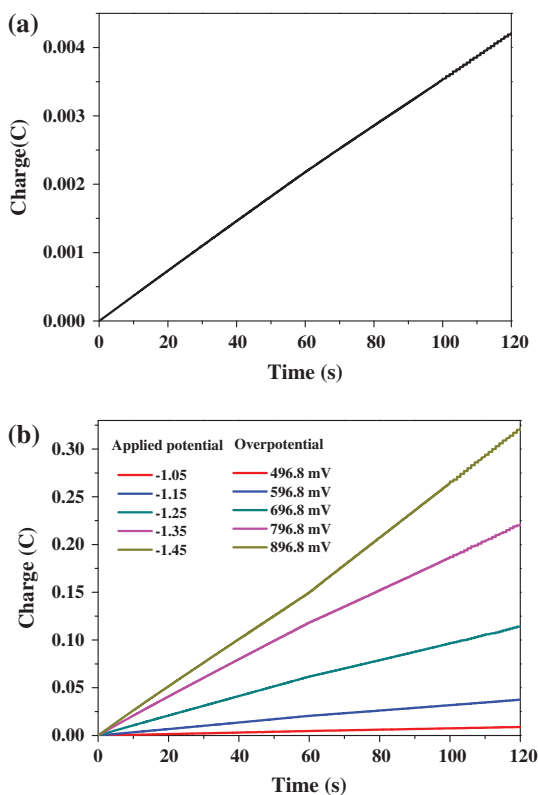


Figure 6. (a) Charge buildup of 0.10 M buffer, pH 7.0. (b) Charge buildup of **1** ($1.75 \mu\text{M}$) vs. a series of applied potentials at pH 7.0. All data have deducted the blank.

current being dependent on the complex concentration could indicate a homogeneous catalyst. Several pieces of evidence also suggest that this iron complex is a homogeneous catalyst: (1) There is no evidence for a heterogeneous electrocatalytic deposit. For example, the electrode was rinsed with water and electrolysis at -1.45 versus Ag/AgCl was run for an additional 2 min in a 0.25 M phosphate buffer at pH 7.0 with no catalyst present in solution. During this period, *ca.* 6 mC of charge was passed, a similar magnitude as is observed for electrolyses conducted with freshly polished electrodes. (2) No discoloration of the electrodes was observed during cyclic voltammetry or bulk electrolysis. To determine whether **1** retains activity over longer time periods, a 72-h CPE at -1.45 V versus Ag/AgCl was conducted in stirred 0.25 M phosphate buffer solutions, pH 7.0, containing **1** (1.75 μ M). After 72 h electrolysis, pH increases by 4.5 units (from 7.0 to 11.5), consistent with accumulation of OH^- by water reduction, $2\text{H}_2\text{O} + 2\text{e}^- \rightarrow \text{H}_2 + 2\text{OH}^-$. As depicted in figure S10, the catalyst affords an essentially linear charge buildup over time, with no substantial loss in activity over 72 h.

4. Conclusion

We describe here a new iron(III) complex that is very easy to obtain from the reaction of simple iron salt and amine-bis(phenolate) ligand. This iron complex can electrocatalyze hydrogen evolution from both acetic acid and water. TOF reaches a maximum of 39.98 at an overpotential of 941.6 mV (in DMF) and 284.29 mol of hydrogen per mole of catalyst per hour at an overpotential of 896.8 mV (in buffer, pH 7.0), respectively. Our ongoing efforts are focused on modifying the Schiff base ligands to give related water-soluble complexes for further studies, with an emphasis on chemistry relevant to sustainable energy cycles.

Supplementary material

CCDC 1044594 contains the supplementary crystallographic data for this paper. This data can be obtained free of charge via <http://www.ccdc.cam.ac.uk/conts/retrieving.html>, or from the Cambridge Crystallographic Data Centre, 12 Union Road, Cambridge CB2 1EZ, UK; Fax: (+44) 1223-336-033; or E-mail: deposit@ccdc.cam.ac.uk.

Disclosure statement

No potential conflict of interest was reported by the authors.

Funding

This work was supported by the National Science Foundation of China [grant number 20971045], [grant number 21271073]; the Student Research Program (SRP) of South China University of Technology.

References

- [1] M.G. Walter, E.L. Warren, J.R. McKone, S.W. Boettcher, Q.X. Mi, E.A. Santori, N.S. Lewis. *Chem. Rev.*, **110**, 6446 (2010).
- [2] H.M. Chen, C.K. Chen, R.S. Liu, L. Zhang, J.J. Zhang, D.P. Wilkinson. *Chem. Soc. Rev.*, **41**, 5654 (2012).
- [3] K.A. Vincent, A. Parkin, F.A. Armstrong. *Chem. Rev.*, **107**, 4366 (2007).
- [4] J.W. Tye, M.B. Hall, M.Y. Darensbourg. *Proc. Nat. Acad. Sci. USA*, **102**, 16911 (2005).
- [5] P.M. Vignais, B. Billoud. *Chem. Rev.*, **107**, 4206 (2007).
- [6] C.J. Pickett, C. Tard. *Chem. Rev.*, **109**, 2245 (2009).
- [7] J.P. Cao, T. Fang, L.Z. Fu, L.L. Zhou, S.Z. Zhan. *Int. J. Hydrogen Energy*, **39**, 10980 (2014).
- [8] L.Z. Fu, L.L. Zhou, L.Z. Tang, Y.X. Zhang, S.Z. Zhan. *J. Power Sources*, **280**, 453 (2015).
- [9] Y. Sun, J.P. Bigi, N.A. Piro, M.L. Tang, J.R. Long, C.J. Chang. *J. Am. Chem. Soc.*, **133**, 9212 (2011).
- [10] W.M. Singh, T. Baine, S. Kudo, S. Tian, X.A.N. Ma, H. Zhou, N.J. DeYonker, T.C. Pham, J.C. Bollinger, D.L. Baker, B. Yan, C.E. Webster, X. Zhao. *Angew. Chem. Int. Ed.*, **51**, 5941 (2012).
- [11] B.D. Stubbart, J.C. Peters, H.B. Gray. *J. Am. Chem. Soc.*, **133**, 18070 (2011).
- [12] M.E. Carroll, B.E. Barton, T.B. Rauchfuss, P.J. Carroll. *J. Am. Chem. Soc.*, **134**, 18843 (2012).
- [13] F. Quentel, G. Passard, F. Gloaguen. *Energy Environ. Sci.*, **5**, 7757 (2012).
- [14] A.D. Nguyen, M.D. Rail, M. Shanmugam, J.C. Fettinger, L.A. Berben. *Inorg. Chem.*, **52**, 12847 (2013).
- [15] J.P. Cao, T. Fang, Z.Q. Wang, Y.W. Ren, S.Z. Zhan. *J. Mol. Catal. A: Chem.*, **391**, 191 (2014).
- [16] L.Z. Fu, T. Fang, L.L. Zhou, S.Z. Zhan. *RSC Adv.*, **4**, 53674 (2014).
- [17] J.P. Cao, T. Fang, L.Z. Fu, L.L. Zhou, S.Z. Zhan. *Int. J. Hydrogen Energy*, **39**, 13972 (2014).
- [18] T. Fang, L.L. Zhou, L.Z. Fu, S.Z. Zhan, Q.Y. Lv. *Polyhedron*, **85**, 355 (2015).
- [19] L.L. Zhou, T. Fang, J.P. Cao, Z. Zhu, X. Su, S.Z. Zhan. *J. Power Sources*, **273**, 298 (2015).
- [20] T. Fang, W. Li, S.Z. Zhan, X. Wei. *J. Coord. Chem.*, **68**, 573 (2015).
- [21] H.I. Karunadasa, C.J. Chang, J.R. Long. *Nature*, **464**, 1329 (2010).
- [22] J.P. Cao, L.L. Zhou, L.Z. Fu, J.X. Zhao, H.X. Lu, S.Z. Zhan. *Catal. Commun.*, **57**, 1 (2014).
- [23] T. Fang, H. Lu, J. Zhao, S.Z. Zhan. *Inorg. Chem. Commun.*, **51**, 66 (2015).
- [24] J.P. Cao, L.-L. Zhou, L.L. Fu, S. Zhan, S.Z. Zhan. *J. Power Sources*, **272**, 169 (2014).
- [25] J.P. Cao, T. Fang, L.L. Zhou, L.Z. Fu, S.Z. Zhan. *Electrochim. Acta*, **147**, 129 (2014).
- [26] J.L. Fillol, Z. Codolà, I. Garcia-Bosch, L. Gómez, J.J. Pla, M. Costas. *Nat. Chem.*, **3**, 807 (2011).
- [27] R. Sarma, A.M. Angeles-Boza, D.W. Brinkley, J.P. Roth. *J. Am. Chem. Soc.*, **134**, 15371 (2012).
- [28] G. Chen, L. Chen, S. Ng, W. Man, T. Lau. *Angew. Chem. Int. Ed.*, **52**, 1789 (2013).
- [29] M.K. Coggins, M. Zhang, A.K. Vannucci, C.J. Dares, T.J. Meyer. *J. Am. Chem. Soc.*, **136**, 5531 (2014).
- [30] Z.-Q. Wang, Z.-C. Wang, S.-Z. Zhan, J.-S. Ye. *Appl. Catal. A*, **490**, 128 (2015).
- [31] G.P. Connor, K.J. Mayer, C.S. Tribble, W.R. McNamara. *Inorg. Chem.*, **53**, 5408 (2014).
- [32] R.R. Chowdhury, A.K. Crane, C. Fowler, P. Kwong, C.M. Kozak. *Chem. Commun.*, 94 (2008).
- [33] G.M. Sheldrick. *SADABS, Program for Empirical Absorption Correction of Area Detector Data*, University of Göttingen, Göttingen, Germany (1996).
- [34] G.M. Sheldrick. *SHELXS 97, Program for Crystal Structure Refinement*, University of Göttingen, Göttingen, Germany (1997).
- [35] M. Velusamy, M. Palaniandavar, R.S. Gopalan, G.U. Kulkarni. *Inorg. Chem.*, **42**, 8283 (2003).
- [36] R. Viswanathan, M. Palaniandavar, T. Balasubramanian, T.P. Muthiah. *Inorg. Chem.*, **37**, 2943 (1998).
- [37] G.P. Connor, K.J. Mayer, C.S. Tribble, W.R. McNamara. *Inorg. Chem.*, **53**, 5408 (2014).